Monthly Notices
of the
ROYAL ASTRONOMICAL SOCIETY

MNRAS **452,** 838–844 (2015) doi:10.1093/mnras/stv1303

Optical observations of an SN 2002cx-like peculiar supernova SN 2013en in UGC 11369

Zheng-Wei Liu,[1⋆] J.-J. Zhang,[2,3⋆] F. Ciabattari,[4⋆] L. Tomasella,[5] X.-F. Wang,[6] X.-L. Zhao,[6] T.-M. Zhang,[7,8] Y.-X. Xin,[2,3] C.-J. Wang[2,3] and L. Chang[2,3]

[1]*Argelander-Institut für Astronomie, Auf dem Hügel 71, D-53121 Bonn, Germany*
[2]*Yunnan Observatories, Chinese Academy of Sciences (CAS), Kunming 650011, People's Republic of China*
[3]*Key Laboratory for the Structure and Evolution of Celestial Object, CAS, Kunming 650011, People's Republic of China*
[4]*Monte Agliale Observatory, Borgo a Mozzano, I-55023 Lucca, Italy*
[5]*INAF, Osservatorio Astronomico di Padova, I-35122 Padova, Italy*
[6]*Physics Department and Tsinghua Center for Astrophysics (THCA), Tsinghua University, Beijing 100084, China*
[7]*National Astronomical Observatories of China (NAOC), Chinese Academy of Sciences, Beijing 100012, China*
[8]*Key Laboratory of Optical Astronomy, National Astronomical Observatories, Chinese Academy of Sciences, Beijing 100012, China*

Accepted 2015 June 9. Received 2015 May 13; in original form 2015 March 20

ABSTRACT

We present optical observations of an SN 2002cx-like supernova SN 2013en in UGC 11369, spanning from a phase near maximum light ($t = +1$ d) to $t = +60$ d with respect to the R-band maximum. Adopting a distance modulus of $\mu = 34.11 \pm 0.15$ mag and a total extinction (host galaxy+Milky Way) of $A_V \approx 1.5$ mag, we found that SN 2013en peaked at $M_R \approx -18.6$ mag, which is underluminous compared to the normal SNe Ia. The near maximum spectra show lines of Si II, Fe II, Fe III, Cr II, Ca II and other intermediate-mass and iron group elements which all have lower expansion velocities (i.e. $\sim$6000 km s^{-1}). The photometric and spectroscopic evolution of SN 2013en is remarkably similar to those of SN 2002cx and SN 2005hk, suggesting that they are likely to be generated from a similar progenitor scenario or explosion mechanism.

Key words: supernovae: general – supernovae: individual: SN 2013en – galaxies: individual: UGC 11369.

1 INTRODUCTION

Type Ia supernovae (SNe Ia) have been successfully used as standardizable candles to measure expansion rate of the Universe (Riess et al. 1998; Perlmutter et al. 1999). Most SNe Ia (about 70 per cent) belong to 'normal' type (Branch, Fisher & Nugent 1993; Li et al. 2003a), they can be calibrated by an empirical relation between their peak luminosities and light-curve shapes (Phillips 1993). However, a new peculiar sub-class of SNe Ia, named Type Iax supernovae (SNe Iax, see Foley et al. 2013) after its prototypical member SN 2002cx (Li et al. 2003a), has been discovered to deviate significantly from this relation. SNe Iax are suggested to arise from thermonuclear explosions of carbon–oxygen white dwarfs (CO WDs) because their maximum-light spectra seem to show signs of CO burning as in normal SNe Ia (Foley et al. 2013). Nevertheless, a core-collapse scenario has been suggested for at least one such type of explosion, i.e. SN 2008ha (Valenti et al. 2008; Foley et al. 2010; Moriya et al. 2010).

SNe Iax have several observational similarities to normal SNe Ia, but also present sufficiently distinct observational properties: (i) their ejecta are dominated by intermediate-mass elements (IMEs) and iron-group elements (Foley et al. 2013). Also, strong mixing with both IMEs and iron-group elements is seen in all layers of the ejecta (Jha et al. 2006; Phillips et al. 2007; Foley et al. 2013). These features are in clear contrast to normal SNe Ia, which are characterized by strongly layered ejecta (Mazzali et al. 2007). (ii) Comparing to normal SNe Ia, SNe Iax are significantly fainter (Foley et al. 2013, 2014). SNe Iax have a wide range in explosion energies (10^{49}–10^{51} erg), ejecta masses (0.15–0.5 $M_\odot$) and ^{56}Ni masses (0.003–0.3 $M_\odot$). (iii) The spectra of SNe Iax are characterized by lower expansion velocities (2000–8000 km s^{-1}) than those of normal SNe Ia ($\approx$1–2 $\times$ 10^4 km s^{-1}) at similar epochs. (iv) Instead of entering a nebular phase dominated by broad forbidden lines of iron-peak elements in normal SNe Ia, the late-time spectra of SNe Iax are dominated by narrow permitted Fe II (Jha et al. 2006). (v) Two SNe Iax (SN 2004cs and SN 2007J) were identified with

⋆ E-mail: zwliu@astro.uni-bonn.de (Z-WL); jujia@ynao.ac.cn (J-JZ); fabciaba@alice.it (FC)

strong He lines in their spectra (Foley et al. 2009, 2013). However, no He lines have yet been detected in spectra of normal SNe Ia.

Li et al. (2011) suggested SN 2002cx (or SNe Iax) are perhaps the most common type of peculiar SNe Ia (see also Foley et al. 2013). It has been estimated that SNe Iax can contribute about 5–30 per cent of the total SN Ia rate (Li et al. 2011; Foley et al. 2013; White et al. 2015). By studying the properties of the host galaxies of SNe Iax, it is found that the host-galaxy morphology distribution of 02cx-like SNe Ia is highly skewed to late-type galaxies, with none of the present sample of 02cx-like SNe Ia occurring in an elliptical galaxy (Foley et al. 2013; Lyman et al. 2013; White et al. 2015). However, at least one SN Iax event (SN 2008ge) is hosted by an S0 galaxy with no signs of star formation. Recently, by analysing pre- and post-explosion *HST* images of some SNe Iax (Foley et al. 2014, 2015; McCully et al. 2014) and considering the He lines seen in two SN Iax spectra, a relatively young age was suggested (< 500 Myr, see Foley et al. 2014) for the progenitor systems of SNe Iax.

Despite recent progress on both, the theoretical and observational side (e.g. see Branch et al. 2004; Jha et al. 2006; Phillips et al. 2007; Valenti et al. 2008, 2009; Foley et al. 2009, 2012, 2013; Moriya et al. 2010; Shen et al. 2010; Kromer et al. 2013, 2015; Liu et al. 2013, 2015; Stritzinger et al. 2014), the problem of progenitors of SNe Iax is still poorly constrained. Theoretically, the hydrodynamical simulations have shown that weak deflagrations of the Chandrasekhar-mass (Ch-mass) CO WDs (Jordan et al. 2012; Kromer et al. 2013; Fink et al. 2014) and Ch-mass hybrid WDs (Kromer et al. 2015) seem to provide a viable physical scenario for SNe Iax. Observationally, a possible progenitor system of one SN Iax event, SN 2012Z, was first detected by McCully et al. (2014). It is further suggested that the SN 2012Z likely had a progenitor system which contained a non-degenerate He-star companion (McCully et al. 2014; Stritzinger et al. 2014). However, the same analyses for pre-explosion *HST* images of other SNe Iax seem to indicate that SNe Iax must have a diverse set of progenitor systems (Foley et al. 2014, 2015). Future observations providing a bigger sample of SNe Iax and more detailed modelling for various theoretical progenitor scenarios will be very helpful for constraining the nature of SN Iax progenitors. To date, no single published model has been found to be able to explain all the observational features and full diversity of SNe Iax, a combination of several progenitor scenarios might be an alternative way to explain the properties of the different observed events within SNe Iax.

In this work, we present optical observations and analysis of a 2002cx-like SN 2013en. The paper is organized as follows. Observations and data reductions are described in Section 2. In Section 3, we performed the analysis of the LCs and spectra of SN 2013en, respectively. A comparison with SN 2002cx, SN 2005hk, and other SNe Ia are also presented in this section. A simple discussion about the possible progenitor systems of SNe Iax and a summary of the main results of this paper are given in Section 4.

2 OBSERVATIONS AND DATA REDUCTION

SN 2013en (= PSN J18513735+2338206) in UGC 11369 was discovered (Ciabattari et al. 2013) in an unfiltered CCD image (limiting magnitude of 19.5 mag) taken by a 0.5 m Newtonian telescope in the course of the Italian Supernovae Search Project (ISSP)[1] on July 30.98 UT. Its J2000.0 coordinates are R.A. = $18^{h}51^{m}37\overset{s}{.}35$, Dec. = $+23^{d}38'20\overset{''}{.}6$, located at 6″ west and 17″ north of the centre of the galaxy UGC 11369 (see Fig. 1).

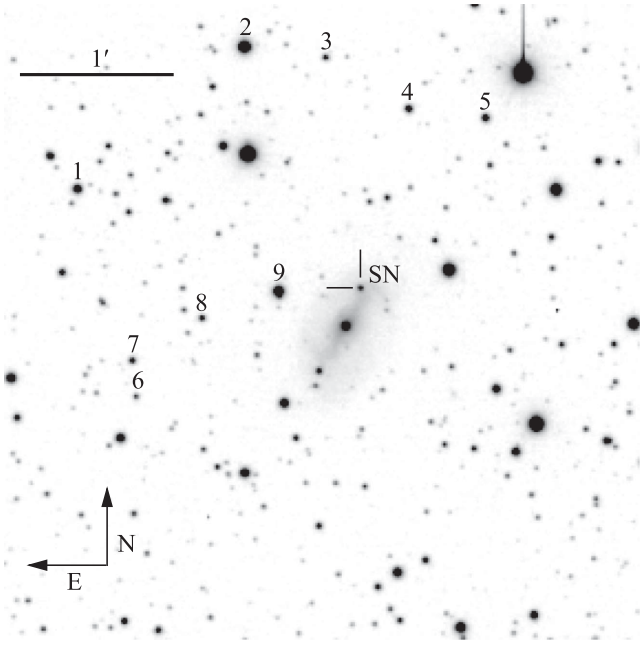

Figure 1. The LJT *R*-band image of SN 2013en and its reference stars, taken on 2013 Aug. 3.61. The image scale is 0.283 arcsec pixel^{-1}. Nine local standard stars are labelled with Arabic numerals.

Shortly after the discovery, SN 2013en was classified as a peculiar SN Ia by Padova–Asiago Supernova Group (Ciabattari et al. 2013; Tomasella et al. 2014) from an optical spectrum (range 340–820 nm) obtained on July 31.84 UT with the Asiago 1.82-m Copernico telescope (+AFOSC).[2] With the supernova identification tool of GELATO (Harutyunyan et al. 2008) and SNID (Blondin & Tonry 2007), a good match between SN 2013en and a typical SN Iax SN 2005hk is found by adopting the redshift $z = 0.015\,207$ of the host galaxy of SN 2013en.

Most optical photometry of SN 2013en was obtained in broad *BVRI* bands with the Yunnan Faint Object Spectrograph and Camera (YFOSC; Zhang et al. 2014) on Li Jiang 2.4-m Telescope (LJT) of Yunnan observatories (YNAO), which started on 2013 Aug. 3. All the CCD images were corrected for bias, flat-field, and cleaned of cosmic rays, using the IRAF package.[3] Since SN 2013en located within the host galaxy, special care is required in the measurement of the instrumental magnitude of the supernova. Therefore, the template subtraction was applied by using the LJT observations obtained on 2014 October 23.50 UT when the SN faded away. The instrumental magnitude measured by subtraction were converted to the standard Johnson *BV* (Johnson et al. 1966) and Kron–Cousins *RI* (Cousins 1981) systems through transformations established by observing (Landolt 1992) standards during photometric nights. The averaged value of the photometric zero-points, determined on two photometric nights, was used to calibrate the local standard stars in the field of SN 2013en. Table 1 lists the standard *BVRI* magnitudes and the corresponding uncertainties of nine local standard stars

[1] http://italiansupernovae.org

[2] http://sngroup.oapd.inaf.it

[3] IRAF, the Image Reduction and Analysis Facility, is distributed by the National Optical Astronomy Observatory, which is operated by the Association of Universities for Research in Astronomy(AURA), Inc. under cooperative agreement with the National Science Foundation (NSF).

Table 1. Magnitudes of the photometric standards in the field of SN 2013en.

Star	*B*(mag)	*V*(mag)	*R*(mag)	*I*(mag)
1	16.150(005)	15.417(003)	14.966(004)	14.646(002)
2	15.310(003)	13.887(002)	13.093(002)	12.454(001)
3	18.219(025)	17.175(012)	16.569(008)	16.052(007)
4	17.577(015)	16.329(006)	15.591(005)	14.989(003)
5	16.824(008)	16.027(005)	15.542(005)	15.043(003)
6	18.636(030)	17.739(015)	17.206(010)	16.785(008)
7	17.672(018)	16.781(008)	16.274(006)	15.838(006)
8	18.376(025)	17.187(012)	16.511(008)	15.988(006)
9	15.545(004)	14.448(002)	13.804(002)	13.204(002)

Note. (1) The finder chart of SN 2013en and nine comparison local stars are shown in Fig. 1. (2) Uncertainties, in units of 0.01 mag, are 1σ.

labelled in Fig. 1. The magnitudes of these stars were then used to transform the instrumental magnitudes of SN 2013en to those of the standard *BVRI* system. Table 2 lists the final flux-calibrated magnitudes of SN 2013en. A single-epoch *VRI*-photometry of SN 2013en obtained on 2013 Jul. 31 with the Asiago 1.82-m Copernico telescope is also listed in Table 2.

A journal of the spectroscopic observations of SN 2013en is given in Table 3. A total of eight low-resolution spectra obtained with the 2.4-m telescope (+YFOSC) at Lijiang Observatory (hereafter LJT), and the 2.16-m telescope (+BFOSC) at Xinglong Observatory (hereafter XLT). A spectrum taken on 2013 Jul. 31 with the 1.82-m Copernico telescope (+AFOSC) at Asiago Observatory (hereafter ACT) is also included in the analysis. All spectra were reduced using standard IRAF routines. Flux calibration of the spectra was performed by means of spectrophotometric standard stars (i.e. LTT-1020) observed at similar air mass on the same night as the SN. With our own routines, the extracted, wavelength-calibrated spectra were corrected for continuum atmospheric extinction using mean extinction curves for Li Jiang and Xinglong Observatories. Additionally, telluric lines have been removed from the data.

3 ANALYSIS

3.1 Light curves

The host galaxy of SN 2013en, UGC 11369, is an SBa galaxy with a recession velocity of 4559 ± 35 km s^{-1} (Falco et al. 1999). Adopting a Λ-cold-dark-matter cosmological model with parameters $\Omega_\Lambda = 0.73$, $\Omega_m = 0.27$, $H_0 = 73 \pm 5$ km s^{-1} Mpc^{-1}, the virgo infall distance of UGC 11369 is $D = 66.2 \pm 4.7$ Mpc ($\mu = 34.11 \pm 0.15$ mag), which will be adopted in this work in the calculations of the luminosity of SN 2013en. The redshift of the UGC 11369 of z= 0.015 207 is used as the redshift of SN 2013en.

The observed *BVRI* LCs are presented in Fig. 2. Unfortunately, our photometry data of SN 2013en are quite sparse and the photometry observations began after the maximum light. Therefore, the maximum-light date of SN 2013en cannot be directly determined by only using our filtered data. To complement the early photometric points we combined the early-time unfiltered data of SN 2013en with our *R*-band light-curve data which is shown in Fig. 2. The unfiltered images were obtained during automatic surveys at Monte Agliale Observatory in the framework of the ISSP.[4] However, there might be possible differences between the ISSP unfiltered magnitudes and our *R*-band results. Fortunately, Zheng et al. (2013) did a detailed comparison for unfiltered magnitudes from ISSP and the standard broad *R*-band magnitudes. They found that these magnitudes are comparable within an uncertainty of 5 per cent (see Li et al. 2003b; Zheng et al. 2013). Therefore, it is reasonable to combine the ISSP unfiltered and our standard *R*-band results.

For comparison, the *BVRI* LCs of SNe 2002cx (see Li et al. 2003a) and 2005hk (which is a well-observed SN that is extremely similar to SN 2002cx, see Phillips et al. 2007) overplotted in Fig. 2. The LCs of the comparison sample have been shifted in peak magnitudes and maximum-light time to match SN 2013en. As shown in Fig. 2, the LCs of SN 2013en seem to follow the photometric evolution seen in SNe 2002cx and 2005hk. In addition, it is shown that the SN 2013en likely peaked in the *R* band at around 2013 July 30 (MJD 56503.8 ± 1.8).

Fig. 3 shows that SN 2013en likely peaked at $m_R \sim 16.7 \pm 0.2$ mag in the *R* band. By adopting a distance modulus of $\mu = 34.11 \pm 0.15$ mag and considering the total extinction of host galaxy and Milky Way (see Section 3.2), we obtain that SN 2013en peaked at $M_R \approx -18.6$ mag (with a total uncertainty of ~0.3–0.4 mag), comparable to SN 2002cx ($M_R \approx -17.6$ mag; Li et al. 2003a) and SN 2005hk ($M_R \approx -18.3$ mag; see Phillips et al. 2007). The uncertainty in this measurement is relatively large due to poorly-sampled LCs at around the maximum light and uncertainties in distance and extinction correction.

3.2 Spectra

Fig. 3 shows time series of our spectra covering the evolution of SN 2013en from around maximum light to two months after maximum light. Note that the spectrum at $t \approx +4$ d was compounded by the spectra obtained by the blue and red grisms. It is shown that the spectra of SN 2013en remain almost unchanged during a period from day +14 to +29 and the spectrum of day +60 is very similar to that of day +45. The 2013en spectrum exhibits strong Na I D interstellar absorption from both the Galactic and host-galaxy components (see the inset of Fig. 3). The equivalent width (EW) of Na I D absorption is suggested to be correlated with the line-of-sight reddening, but with a large scatter (e.g. Turatto, Benetti & Cappellaro 2003; Poznanski, Prochaska & Bloom 2012). The Na I D absorption due to the host galaxy of SN 2013en is measured to be about 1.62 Å at $t \approx +4$ d, which corresponds to a possible host galaxy reddening $E(B-V)_{host} = 0.26 \pm 0.03$ mag (Turatto et al. 2003; Poznanski et al. 2012). The Milky Way reddening is $E(B-V)_{Gal} = 0.254$ mag, according to Schlegel, Finkbeiner & Davis (1998). Therefore, a total reddening (host galaxy+Milky Way) of $E(B-V)_{tot} \approx 0.5$ mag is adopted for SN 2013en in this paper. And a reddening law with $R_V = 3.1$ of Cardelli, Clayton & Mathis (1989) is assumed for the extinction correction.

In Fig. 4, we compare the spectra SN 2013en with those of SN 2002cx and SN 2005hk (02cx-like), SN 1999ac (a 1991T-like) and SN 2003du (a normal SN Ia) at similar phases. No signatures of hydrogen and helium are found in spectra of SN 2013en, which indicates that its progenitor was likely an evolved star (Foley et al. 2012, 2013) or an envelope-stripped star like the Wolf–Rayet star. One can see that the spectra of SN 2013en and their evolution are quite different from those of normal SNe Ia, but are very similar to SN 2002cx and SN 2005hk (Li et al. 2003a; Branch et al. 2004).

A detailed spectra comparison between SN 2013en and SN 2002cx, SN 2005hk (Li et al. 2003a; Branch et al. 2004; Jha et al. 2006; Phillips et al. 2007) is performed at $t = +1$, +29, and +45 d

[4] http://www.oama.it.

Table 2. The *BVRI* photometry of SN 2013en from LJT+YFOSC.

UT Date	MJD	Phase[a]	*B*(mag)	*V*(mag)	*R*(mag)	*I*(mag)	Telescope	Observer
Jul. 31.87	56504.87	1.07	–	17.40(03)	16.74(04)	16.28(04)	ACT+AFOSC	L. Tomasella
Aug. 03.61	56507.61	3.81	18.03(05)	17.35(03)	16.82(03)	16.37(02)	LJT+YFOSC	J. J. Zhang
Aug. 15.73	56519.73	15.93	19.31(08)	17.89(04)	17.13(03)	16.55(03)	LJT+YFOSC	J. J. Zhang
Aug. 17.70	56521.70	17.90	19.42(08)	17.95(04)	17.22(03)	16.62(03)	LJT+YFOSC	J. J. Zhang
Sep. 13.63	56548.63	44.83	20.62(10)	18.91(04)	18.07(04)	17.61(03)	LJT+YFOSC	J. J. Zhang
Sep. 28.51	56563.51	59.71	20.77(10)	19.12(06)	18.42(05)	17.92(03)	LJT+YFOSC	J. J. Zhang
Oct. 09.50	56574.50	70.70	20.94(10)	19.28(06)	18.69(06)	18.19(05)	LJT+YFOSC	J. J. Zhang
Oct. 10.50	56575.50	71.70	21.05(10)	19.32(08)	18.71(07)	18.24(08)	LJT+YFOSC	J. J. Zhang

Notes. Uncertainties, in units of 0.01 mag, are 1σ; MJD = JD−2400000.5.
[a]Relative to the date of *R*-band maximum (MJD = 56503.80).

Table 3. Journal of spectroscopic observations of SN 2013en.

UT Date	MJD (−240000.5)	Epoch[a] (d)	Res (Å pixel^{-1})	Range (Å)	Airmass	Exp.time (s)	Telescope (+facility)	Observer
Jul. 31.85	56504.85	1.05	13.0	3800–8000	1.11	1800	ACT+AFOSC	L. Tomasella
Aug. 02.61	56506.61	2.81	17.5	3500–8900	1.02	1800	LJT+YFOSC	J. J. Zhang
Aug. 03.73	56507.73	3.93	6.7	5000–9800	1.14	2700	LJT+YFOSC	J. J. Zhang
Aug. 03.76	56507.76	3.96	7.5	3800–7200	1.29	2700	LJT+YFOSC	J. J. Zhang
Aug. 09.60	56513.60	9.80	20.3	3500–8800	1.08	3600	XLT+BFOSC	X. F. Wang
Aug. 13.73	56517.73	13.93	17.5	3500–8900	1.29	1800	LJT+YFOSC	J. J. Zhang
Aug. 28.59	56532.59	28.79	17.5	3500–8900	1.01	2700	LJT+YFOSC	J. J. Zhang
Sep. 13.64	56549.14	45.34	17.5	3500–8900	1.01	3600	LJT+YFOSC	J. J. Zhang
Sep. 28.53	56563.53	59.73	17.5	3500–8900	1.04	3600	LJT+YFOSC	J. J. Zhang

Note. [a]Relative to the date of *R*-band maximum (MJD=56503.80).

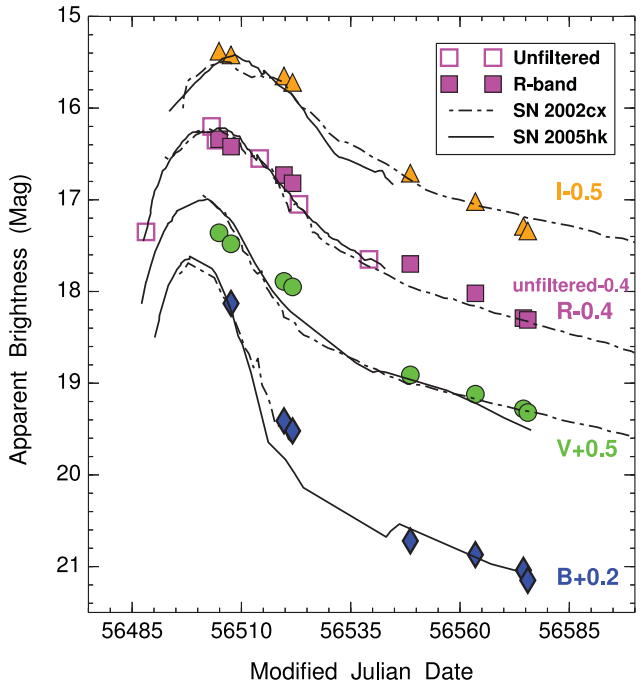

Figure 2. *BVRI* (filled markers) and unfiltered (open squares) light curves (LCs) of SN 20013en. The LCs have been shifted by the amount indicated in the legend. For a comparison, the LCs of SNe 2002cx (*BVRI* band, dash–dotted lines) and 2005hk (*BVRI* band, solid lines) are also shown. The LCs of SNe 2002cx and 2005hk have been shifted to match the light curve of SN 2013en at peak. Here, the uncertainties for data points are smaller than the plotted symbols.

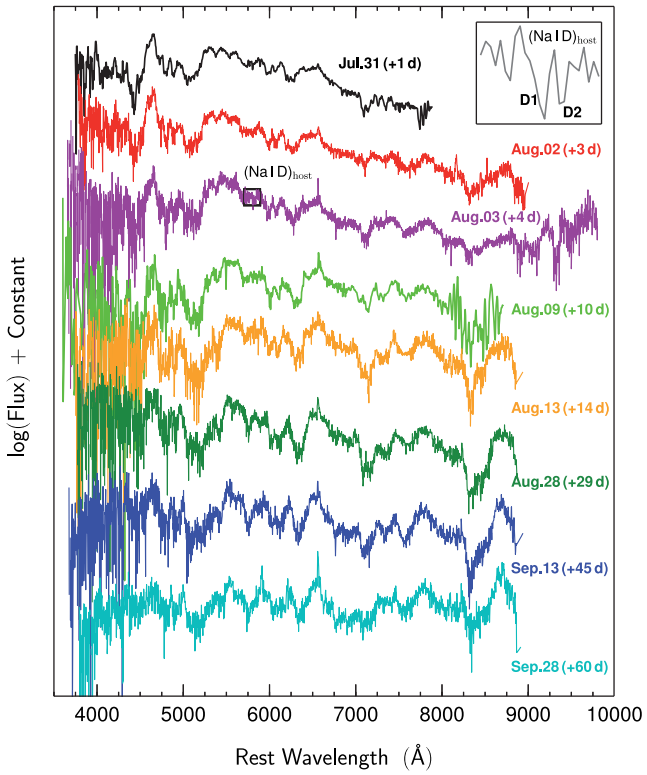

Figure 3. Time evolution of the optical spectra of SN 2013en. The spectra have been corrected for the redshift of the host galaxy. The phases indicated to the right of each spectrum are relative to the *R*-band maximum light. The Na I D absorption of the host galaxy in the spectrum at $t \approx +4$ d is marked with black box and amplified on the top right.

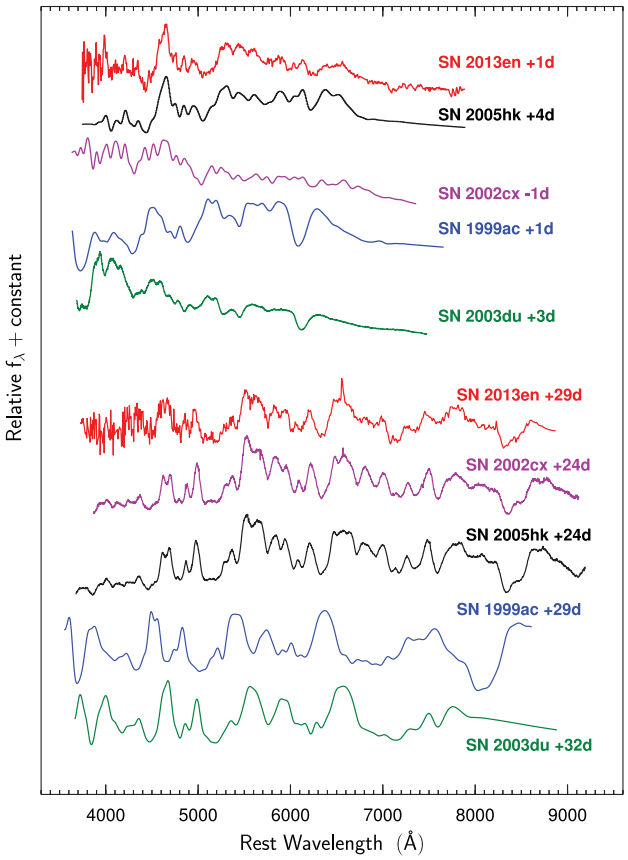

Figure 4. Comparison of spectra of SN 2013en at +1 and +29 d with SN 2002cx (magenta curve), SN 2005hk (black curves), a peculiar, 1991T-like SN Ia (SN 1999ac; blue), and normal SNe Ia (SN 2003du; green) at similar epoch.

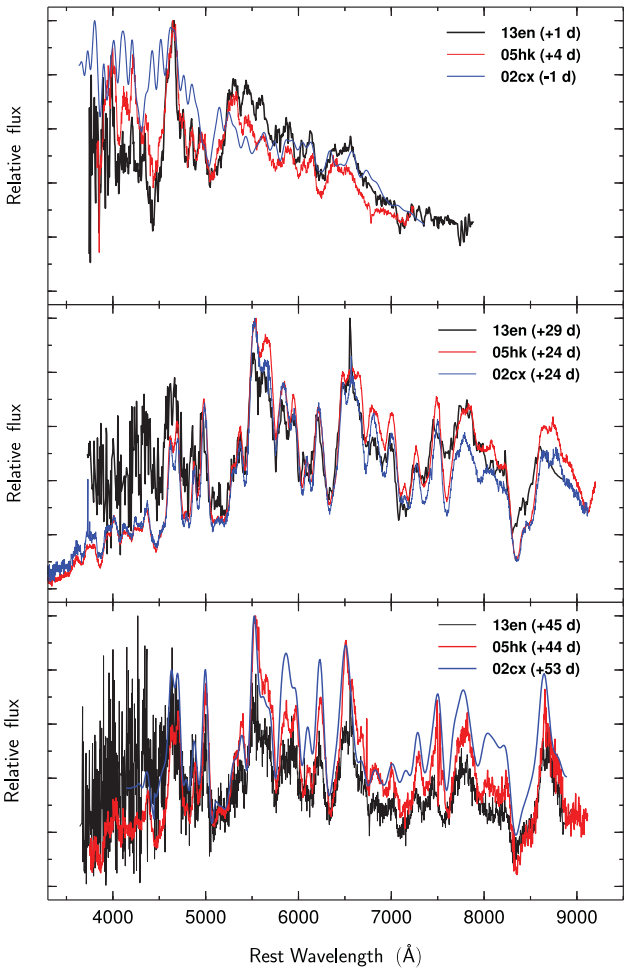

Figure 5. Spectra of SN 2013en taken at +1 (black; top panel), +29 (black; middle panel) and +45 d (black; bottom panel) relative to *R*-band maximum light. Overplotted are the spectra of SN 2002cx (at ∼+10, +24 and +53 d in the top, middle and bottom panels, respectively) and SN 2005hk (at ∼+4, +24 and +44 d in the top, middle and bottom panels, respectively). All of the spectra have been corrected for the redshift of the host galaxy and for the reddening.

after maximum brightness (*R*-band), as shown in Fig. 5. It is found that they are nearly identical, and the line features in SN 2013en spectra closely resemble those of SN 2002cx and SN 2005hk, except for a slight difference in line velocities and widths. Furthermore, the evolution of some typical line features seen in the spectra of SN 2013en are shown in Fig. 6. As it can be seen that the spectra of SN 2013en are dominated by Fe II lines. Also, Co II, Na I and Ca II lines are clearly visible in the spectra. A detailed line identification for the 2002cx-like SNe was addressed in Branch et al. (2004).

3.3 Ejecta velocity

The blueshift of the absorption lines in SN spectra has been used as an indicator of expansion velocity, and they can provide information about the kinetic energy of the SN explosion, the chemical stratification of the ejecta (Parrent, Friesen & Parthasarathy 2014), and even the progenitor environment (Wang et al. 2013). Here, the ejecta velocity of SN 2013en is derived from the absorption features of Ca II and Fe II lines. The location of the blueshifted absorption minimum is measured by using the direct measurement of absorption minima. Fig. 7 shows that the ejecta velocity of SN 2013en measured from the minimum blueshift of Ca II and Fe II evolves from $\simeq 6400\,\mathrm{km\,s^{-1}}$ at $t = +3$ d to $\simeq 5500\,\mathrm{km\,s^{-1}}$ at $t = +60$ d. For a comparison, the ejecta velocities of SN 2002cx, SN 2005hk (Phillips et al. 2007) and SN 2012Z (Stritzinger et al. 2015; Yamanaka et al. 2015) are also plotted in Fig. 7.

Based on the unfiltered and *R*-band light curve presented in Fig. 2, we measured for SN 2013en the decline rate within the first 15 d after the maximum, $\Delta m_{15}(R) = 0.55 \pm 0.18$ mag. The large error is due to a relatively large uncertainty in estimating the date of maximum light (see Section 3.1). Using Arnett (1982) Law, we can derive an ejecta mass-dependent relationship between ejecta velocity and $\Delta m_{15}(R)$ (see also Narayan et al. 2011). In Fig. 8, we present such a relation for SN 2013en and other comparison sample of 02cx-like SNe Ia. It can be seen that the expansion velocity of SN 2013en is significantly slower than that of normal SNe Ia, but the location of SN 2013en in the plot is consistent with that of SN 2002cx and SN 2005hk. Narayan et al. (2011) suggested that the peak luminosities of 02cx-like SNe Ia is related to their ejecta velocities, except for SN 2009ku. It is obvious that SN 2013en is in line with such a relation.

4 DISCUSSION AND CONCLUSION

In this paper, we present optical photometry and spectroscopy of a 02cx-like peculiar supernova SN 2013en. Combining our LCs

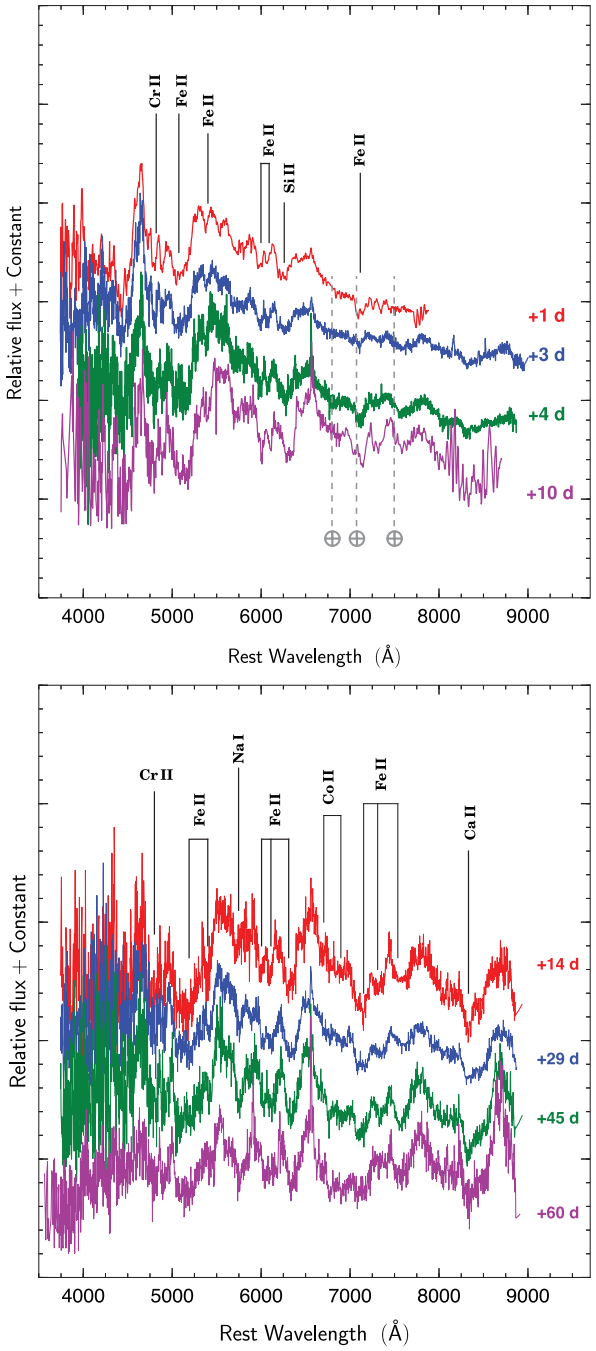

Figure 6. Spectral evolution of SN 2013en. The phases marked are relative to date of R maximum. The spectra have been corrected for the redshift of the host galaxy and for the reddening (assuming $E(B-V)_{\rm tot} \sim 0.5$ mag). Line identification is based on Branch et al. (2004). For clarity the spectra have been shifted vertically, residual telluric absorption lines are marked with '⊕' symbols.

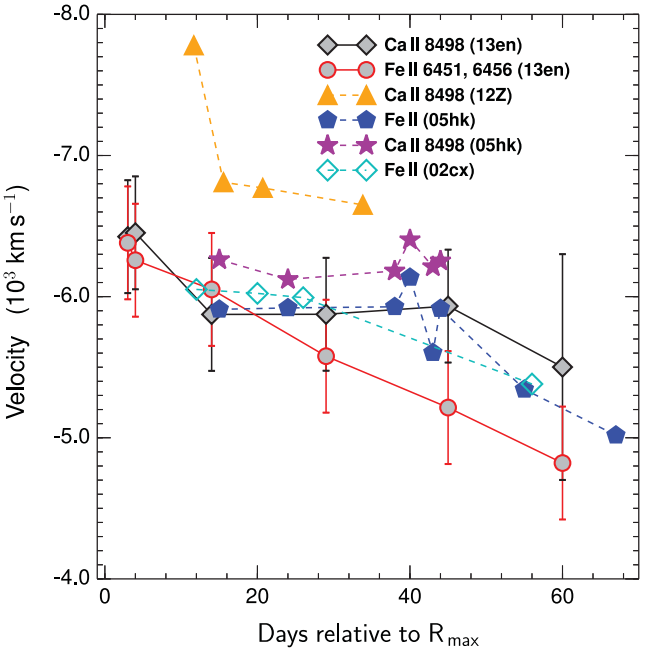

Figure 7. Expansion-velocity evolutions of Ca II and Fe II lines as measured from the spectra of SN 2013en. For a comparison, temporal evolutions of similar lines of SN 2002cx, SN 2005hk and SN 2012Z are also plotted.

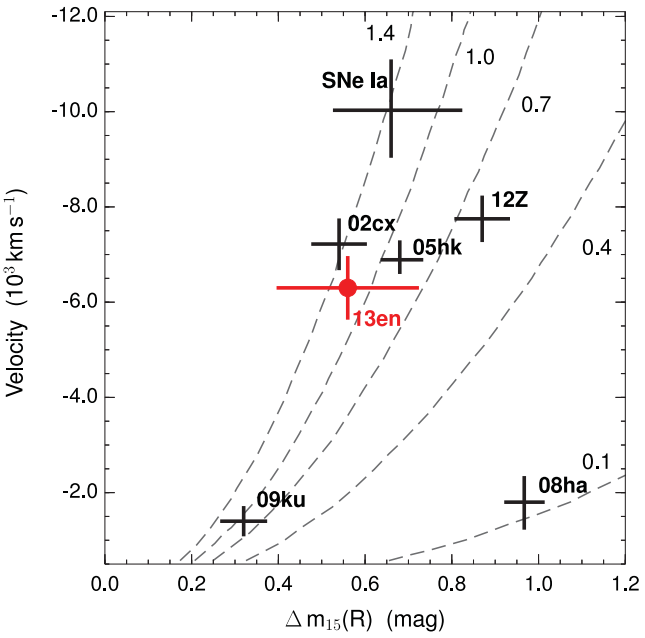

Figure 8. Comparison of $\Delta m_{15}(R)$ and the photospheric velocity at around the maximum light ($t \approx +3$ d) for various objects in the SN 2002cx-like class. The dashed lines represents the relationship between ejecta velocity and Δm_{15} for (from bottom right to top left) 0.1, 0.4, 0.7, 1.0 and 1.4 $M_\odot$ of ejecta mass. SN 2013en is marked with a red filled circle.

and the early-time unfiltered data, we were able to determine that SN 2013en likely peaked in the R band at around 2013 July 30 (MJD = 56503.80), with $m_R \sim 16.7 \pm 0.2$ mag and $\Delta m_{15}(R) = 0.55 \pm 0.18$ mag.

Based on the Na I D absorption from the spectra, we estimated that SN 2013en suffered a total reddening of $E(B-V)_{\rm tot} \approx 0.5$ mag. Assuming a distance modulus $\mu = 34.11 \pm 0.15$ mag, we found that SN 2013en has an absolute peak magnitude of -18.6 mag in the R band. The brightness of SN 2013en is consistent with that of peculiar subluminous SN 2002cx and SN 2005hk.

Besides the photometric evolution, the spectra of SN 2013en are found to show similar features and evolution to those SNe 2002cx and 2005hk. These results indicate that SN 2013en is probably produced from the same progenitor scenario as SNe 2002cx and 2005hk. However, the exact nature of progenitor systems of SNe

Iax remains unclear. The *HST* analysis for one SN Iax SN 2012Z suggests that a binary system consists of a He-star companion and a CO WD is likely to be its progenitor system (McCully et al. 2014). However, the observations for other SN Iax objects also show that a wide variety of progenitor scenario may be realized within the SNe Iax class (Foley et al. 2013, 2014, 2015; Stritzinger et al. 2015).

Theoretically, as mentioned previously, numerical simulations show that weak deflagrations of the Ch-mass CO WDs produce observational characteristics of 2002cx-like SNe Iax quite well (Jordan et al. 2012; Kromer et al. 2013; Fink et al. 2014), although it appears difficult in explaining 2008ha-like SNe Iax (SNe 2008ha and 2010ae, see Valenti et al. 2008; Stritzinger et al. 2014) which have a very low ^{56}Ni mass of $\sim$0.003 $M_{\odot}$. Recently, however, hybrid C-O-Ne Ch-mass WDs have also been suggested likely to trigger weak pure deflagration explosions of SNe Iax (Denissenkov et al. 2015). Because the Hybrid WDs have much lower C to O abundance ratios at the moment of the explosive C ignition than their pure CO counterparts (Denissenkov et al. 2015), which probably will lead to a low ^{56}Ni mass after the SN explosion. Recent hydrodynamical simulations for the weak pure deflagration explosions of a Ch-mass hybrid WD have shown that this specific explosion can explain the observational features of faint SNe Iax such as SN 2008ha (see Kromer et al. 2015). On the other hand, the fallback core-collapse explosions of massive stars were also proposed for the peculiar SN Iax SN 2008ha (see Valenti et al. 2008; Foley et al. 2010; Moriya et al. 2010). Nevertheless, to date, weak deflagration explosions of a Ch-mass WD seem to give better explanations for the observational properties of SNe Iax.

ACKNOWLEDGEMENTS

We acknowledge the anonymous referee for valuable comments that helped us to improve the paper. We also acknowledge the support of the staff of Li-Jiang 2.4-m telescope (LJT) and Xinlong 2.16-m telescope. Funding for the LJT has been provided by Chinese Academy of Science (CAS) and the People's Government of Yunnan Province. Partially based on data obtained in Asiago, by the Copernico 1.82-m telescope operated by INAF OAPd. ZWL is supported by the Alexander von Humboldt Foundation. JJZ is supported by the National Natural Science Foundation of China (NSFC, grant 11403096). LT is partially supported by the PRIN-INAF 2011 with the project 'Transient Universe: from ESO Large to PESSTO'. XFW is supported by the Major State Basic Research Development Program (2013CB834903), the NSFC (grants 11073013, 11178003, 11325313), Tsinghua University Initiative Scientific Research Program and the Strategic Priority Research Program 'The Emergence of Cosmological Structures' of the Chinese Academy of Sciences (grant no. XDB09000000).

REFERENCES

Arnett W. D., 1982, ApJ, 253, 785
Blondin S., Tonry J. L., 2007, ApJ, 666, 1024
Branch D., Fisher A., Nugent P., 1993, AJ, 106, 2383
Branch D., Baron E., Thomas R. C., Kasen D., Li W., Filippenko A. V., 2004, PASP, 116, 903
Cardelli J. A., Clayton G. C., Mathis J. S., 1989, ApJ, 345, 245
Ciabattari F. et al., 2013, Cent. Bur. Electron. Telegrams, 3613, 1
Cousins A. W. J., 1981, South Afr Astron. Obs. Circ., 6, 4
Denissenkov P. A., Truran J. W., Herwig F., Jones S., Paxton B., Nomoto K., Suzuki T., Toki H., 2015, MNRAS, 447, 2696
Falco E. E. et al., 1999, PASP, 111, 438
Fink M. et al., 2014, MNRAS, 438, 1762
Foley R. J. et al., 2009, AJ, 138, 376
Foley R. J. et al., 2010, AJ, 140, 1321
Foley R. J. et al., 2012, ApJ, 753, L5
Foley R. J. et al., 2013, ApJ, 767, 57
Foley R. J., McCully C., Jha S. W., Bildsten L., Fong W.-f., Narayan G., Rest A., Stritzinger M. D., 2014, ApJ, 792, 29
Foley R. J., Van Dyk S. D., Jha S. W., Clubb K. I., Filippenko A. V., Mauerhan J. C., Miller A. A., Smith N., 2015, ApJ, 798, L37
Harutyunyan A. H. et al., 2008, A&A, 488, 383
Jha S., Branch D., Chornock R., Foley R. J., Li W., Swift B. J., Casebeer D., Filippenko A. V., 2006, AJ, 132, 189
Johnson H. L., Mitchell R. I., Iriarte B., Wisniewski W. Z., 1966, Commun. Lunar Planet. Lab., 4, 99
Jordan G. C., IV, Perets H. B., Fisher R. T., van Rossum D. R., 2012, ApJ, 761, L23
Kromer M. et al., 2013, MNRAS, 429, 2287
Kromer M. et al., 2015, MNRAS, 450, 3045
Landolt A. U., 1992, AJ, 104, 340
Li W. et al., 2003a, PASP, 115, 453
Li W., Filippenko A. V., Chornock R., Jha S., 2003b, PASP, 115, 844
Li W. et al., 2011, Nature, 480, 348
Liu Z.-W., Kromer M., Fink M., Pakmor R., Röpke F. K., Chen X. F., Wang B., Han Z. W., 2013, ApJ, 778, 121
Liu Z.-W., Moriya T. J., Stancliffe R. J., Wang B., 2015, A&A, 574, A12
Lyman J. D., James P. A., Perets H. B., Anderson J. P., Gal-Yam A., Mazzali P., Percival S. M., 2013, MNRAS, 434, 527
McCully C. et al., 2014, Nature, 512, 54
Mazzali P. A., Röpke F. K., Benetti S., Hillebrandt W., 2007, Science, 315, 825
Moriya T., Tominaga N., Tanaka M., Nomoto K., Sauer D. N., Mazzali P. A., Maeda K., Suzuki T., 2010, ApJ, 719, 1445
Narayan G. et al., 2011, ApJ, 731, L11
Parrent J., Friesen B., Parthasarathy M., 2014, Ap&SS, 351, 1
Perlmutter S. et al., 1999, ApJ, 517, 565
Phillips M. M., 1993, ApJ, 413, L105
Phillips M. M. et al., 2007, PASP, 119, 360
Poznanski D., Prochaska J. X., Bloom J. S., 2012, MNRAS, 426, 1465
Riess A. G. et al., 1998, AJ, 116, 1009
Schlegel D. J., Finkbeiner D. P., Davis M., 1998, ApJ, 500, 525
Shen K. J., Kasen D., Weinberg N. N., Bildsten L., Scannapieco E., 2010, ApJ, 715, 767
Stritzinger M. D. et al., 2014, A&A, 561, A146
Stritzinger M. D. et al., 2015, A&A, 573, A2
Tomasella L. et al., 2014, Astron. Nachr., 335, 841
Turatto M., Benetti S., Cappellaro E., 2003, in Hillebrandt W., Leibundgut B., eds, From Twilight to Highlight: The Physics of Supernovae. Springer-Verlag, Berlin, p. 200
Valenti S. et al., 2008, MNRAS, 383, 1485
Valenti S. et al., 2009, Nature, 459, 674
Wang X., Wang L., Filippenko A. V., Zhang T., Zhao X., 2013, Science, 340, 170
White C. J. et al., 2015, ApJ, 799, 52
Yamanaka M. et al., 2015, preprint (arXiv:1505.01593)
Zhang J.-J., Wang X.-F., Bai J.-M., Zhang T.-M., Wang B., Liu Z.-W., Zhao X.-L., Chen J.-C., 2014, AJ, 148, 1
Zheng W. et al., 2013, ApJ, 778, L15

This paper has been typeset from a TEX/LATEX file prepared by the author.